OXFORD CDE

Journal of Computational Design and Engineering, 2020, 7(0), 1–12

doi: 10.1093/jcde/qwaa041
Journal homepage: www.jcde.org

RESEARCH ARTICLE

Nonlocal vibration of carbon/boron-nitride nano-hetero-structure in thermal and magnetic fields by means of nonlinear finite element method

Hamid M. Sedighi[1,2,*], Mohammad Malikan[3], Ali Valipour[1] and Krzysztof Kamil Żur[4]

[1]Mechanical Engineering Department, Faculty of Engineering, Shahid Chamran University of Ahvaz, P.O. Box 61357-43337, Ahvaz, Iran; [2]Drilling Center of Excellence and Research Center, Shahid Chamran University of Ahvaz, Ahvaz, Iran; [3]Department of Mechanics of Materials and Structures, Faculty of Civil and Environmental Engineering, Gdansk University of Technology, P.O. Box 80-233, Gdansk, Poland and [4]Faculty of Mechanical Engineering, Bialystok University of Technology, Wiejska 45C Street, 15-351 Bialystok, Poland

*Corresponding author. E-mail: h.msedighi@scu.ac.ir; hmsedighi@gmail.com

Abstract

Hybrid nanotubes composed of carbon and boron-nitride nanotubes have manifested as innovative building blocks to exploit the exceptional features of both structures simultaneously. On the other hand, by mixing with other types of materials, the fabrication of relatively large nanotubes would be feasible in the case of macroscale applications. In the current article, a nonlinear finite element formulation is employed to deal with the nonlocal vibrational behavior of carbon/boron-nitride nano-hetero-tubes in the presence of magneto-thermal environment. Euler–Bernoulli beam model in conjunction with the Eringen's nonlocal theory of elasticity is adopted to derive the governing equation of motion. In order to conduct a nonlinear frequency analysis, the von-Kármán nonlinearity associated with moderate rotations is also considered. It is well known that temperature gradients can significantly change the dynamic behavior of nanotubes. On the other hand, the coefficients of thermal expansions of carbon and boron-nitride nanotubes are quite different that may affect the structural stability of hybrid nanotubes. Hence, to explore the vibration characteristic of such composite structures, the influence of magneto-thermal environment is also taken into account. Finally, the eigenvalue analysis is performed to exhibit the nonlinear mode shapes and natural frequencies of the system due to initial displacement. It is expected that the recognition of dynamic behavior of such hybrid nanotubes may open the doors to the creative design of next-generation nano-devices.

Keywords: hybrid nanotube; nonlinear finite element analysis; magnetic field; nonlocal elasticity; thermal environment

1. Introduction

Following the discovery of carbon and boron-nitride hetero-nanotubes, several researches have been performed on exploring different aspects of such nanocomposite materials in the design of future nanoelectromechanical devices. From a structural point of view, boron-nitride nanotubes (BNNTs) are similar to their counterparts, carbon nanotubes (CNTs), in which carbon atoms are alternately replaced by boron and nitrogen atoms. Nevertheless, it was proved that hexagonal BNNTs are

Received: 26 January 2020; **Revised:** 7 February 2020; **Accepted:** 9 February 2020

much more chemically and thermally stable than CNTs. BNNTs that are a result of wrapping a plate-like boron-nitride sheet to a tubular structure, have different properties compared to CNTs. For example, thanks to the arrangement of their tabular patterns, CNTs may be regarded as a metal or semiconductor material and on the other hand, BNNTs are usually considered as a non-conductive medium. It is well-established that the uniform CNTs have superior magnetic/mechanical/electronic properties that make them a suitable material to be utilized in high-sensitive nanoelectronic devices. BN nanotubes have remarkable thermal properties that make them efficiently applicable in high-temperature mediums as well as biological environments. Such exceptional features of the mentioned nanotubes, i.e. carbon and BNNTs, have encouraged researchers to work on a new class of composites exploiting the properties of both materials, namely carbon/boron-nitride CNTs (C/BNNTs) (Nozaki & Itho, 1996; Stephan et al., 1994).

Inspired by this idea, many engineers and scientists thought of synthesizing C/BN hetero-nanotubes to produce the next-generation of smart/intelligent nano-devices. Moreover, very often they are encouraged to employ this kind of nanocomposite material in different environmental and physical conditions. Rodríguez Juárez, Anota, Cocoletzi, Sánchez Ramírez, and Castro (2017) reported the mechanical, magnetic and electronic properties of different combinations of C-BNNTs and proposed them for utilizing in drug delivery systems as well as nano-vehicles. The transport features and conductance of a hetero-structure made up of carbon and BNNTs were investigated by Xiao, Zhang, Zhang, Sun, and Zhong (2013). In another work, on the basis of molecular dynamics (MD) simulations and continuum elasticity theory, the occurrence of a beat phenomenon in analyzing the natural frequencies of a BN-CNT was reported by Zhang and Wang (2017). They emphasized that the essential difficulties in producing mass detectors for atomic-scale measuring may be resolved by the interaction between two vibration modes of the hetero-nanotubes. Based on the non-equilibrium Green's function assumptions, a theoretical investigation on the C-BN-C nanotubes was performed by Vedaei and Nadimi (2019) where the tendency of NO_2 and O_2 molecules toward a chemical attachment with the surface of the hetero-nanotube was demonstrated. Within the framework of molecular mechanics theory, Chen et al. (2019) theoretically identified the prominent thermal rectification (TR) impacts of a rectifier-based C/BN nanotube and investigated the thermal transport across its interface. Moreover, it was demonstrated that when the system is subjected to a high-temperature bias, the armchair hetero-nanotubes have less TR ratio than that of zigzag C/BN ones. With the help of MD simulations, Badjian and Setoodeh (2017) utilized a boron nitride nanotube to coat a defected CNT and enhanced the tensile and buckling behavior of the homogenous nanotube. They demonstrated that while atom vacancies considerably affect the buckling behavior of CNTs, the presence of BNNT coating results in improving the mechanical strength of such nanotubes. On the basis of Morse and cosine potential functions, Genoese, Genoese, and Salerno (2019) analyzed the nanoscale behavior of single-walled silicon carbide (SiC), boron-nitride (BN), and carbon (C) nanotubes using MD. Both armchair and zigzag patterns were considered and the elastic properties of the studied nanotubes were evaluated by means of Donnell thin shell theory. With the aid of MD simulations, the modal participation of a doubly-clamped single-walled CNTs in the presence of vacancies was studied by Eltaher, Almalki, Almitani, Ahmed, and Abdraboh (2019). In another investigation, on the basis of continuum mechanics, Eltaher, Omar, Abdalla, and Gad (2019) presented the nonlocal static bending and vibrational analysis of a nanobeam assuming the effects of piezoelectricity and surface energies, employed the finite element formulation to discretize the governing equations, and obtained the numerical solution of the problem. The nonlocal natural frequencies of a hinged-hinged hybrid nanotube were studied by Cheng et al. (2019). They found the numerical solution of the harvested equations by means of dynamic stiffness technique and exhibited that the considered nanotube becomes more unstable at larger values of nonlocal and length ratio parameters. Plenty of research works have been recently conducted in the case of hybrid/homogeneous nanostructures that are not reported here, for the sake of brevity (Agwa & Eltaher, 2016; Ansari, Gholami, & Ajori, 2013; Barretta, Čanadija, & Marotti de Sciarra, 2016, 2019; Barretta, Faghidian, Marotti de Sciarra, & Pinnola, 2019; Barretta & Marotti de Sciarra, 2019; Chang, 2017; Choyal, Choyal, Nevhal, Bergaley, & Kundalwal, 2019; Eltaher, Abdraboh, & Almitani, 2018; Eltaher & Agwa, 2016; Eltaher, Almalki, Ahmed, & Almitani, 2019; Eltaher, Almalki, Almitani, & Ahmed, 2019; Eltaher, El-Borgi, & Reddy, 2016; Eltaher, Khater, Abdel-Rahman, & Yavuz, 2014; Eltaher, Khater, & Emam, 2016; Eltaher, Mohamed, Mohamed, & Seddek, 2019; Emam, Eltaher, Khater, & Abdalla, 2018; Ghalambaz, Ghalambaz, & Edalatifar, 2015, 2016; Hamed, Sadoun & Eltaher, 2019; Jena, Chakraverty, & Malikan, 2019; Jena, Chakraverty, Malikan, & Tornabene, 2019; Malikan, 2017, 2018, 2019a, 2019b; Malikan, Dimitri, & Tornabene, 2019; Malikan & Nguyen, 2018a; Malikan, Nguyen, Dimitri, & Tornabene, 2019; Malikan, Nguyen, & Tornabene, 2018a, 2018b; Mohamed, Eltaher, Mohamed, & Seddek, 2019; Noghrehabadi, Eslami, & Ghalambaz, 2013; Noghrehabadi, Ghalambaz, & Ghanbarzadeh, 2012; Ouakad & Sedighi, 2016; Ramezannejad Azarboni, 2019; Sedighi, 2014; Sedighi & Bozorgmehri, 2016; Yazdanpanahi, Noghrehabadi, & Ghalambaz, 2014; Yazdanpanahi, Noghrehabadi, & Ghanbarzadeh, 2013; Zhao, Zhang, & Lie, 2018; Zhen, Wen, & Tang, 2019; Zhu, Chen, Dong, & Li, 2019).

It is demonstrated that the homogenous nanotubes such as CNTs and BNNTs, could be solely utilized in miniature electronic/magnetic devices. As mentioned above, however, the inspiring idea is to exploit the advantages of both materials at the same time by producing an innovative nano-hetero-structure composed of CNTs/BNNTs for the next-generation nanotubes. Following this concept, the present study deals with the nonlinear vibrational behavior of a size-dependent carbon/boron-nitride hetero-nanotube incorporating Euler–Bernoulli (EB) beam model and Eringen's nonlocal theory of elasticity. As the dimensions of a structure diminish to sub-micron scales, size-dependent elasticity theories should be taken into consideration to predict more precise behavior of such structures. To this end, the nonlocal elasticity theory is included in the governing equation of motion. The magneto-thermal environment surrounds the hetero-nanotube and the effects of nonlocality, initial amplitude and length ratio parameter are investigated here through a nonlinear finite element analysis. The obtained results are justified in comparison with those reported in the literature.

2. Mathematical Formulation

Figure 1 illustrates a doubly clamped nano-hetero-structure made of two kinds of tubular materials. The first part of the considered composite (hybrid) nanotube is a homogenous CNT and the second part is a BNNT. It is assumed that two parts possess identical geometrical properties with different material constants. The total length of the hetero-nanotube is L while the lengths of the two segments are $L_1 = \xi L$, $0 < \xi < 1$, and $L_2 = (1 - \xi)L$, as shown in Fig. 1. Adopting Maxwell's law

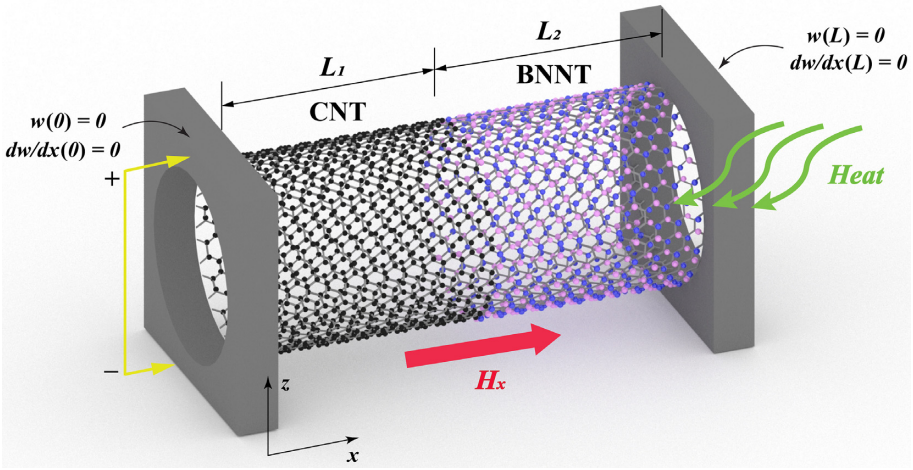

Figure 1: The schematic configuration of a doubly clamped nano-hetero-structure made of a C/BN nanotubes.

assumptions, the presence of a magnetic field in the space induces a force whose direction is perpendicular to the magnetic field. Thereby, an axial magnetic field H_x generates a transversal membrane force called Lorentz force. It is assumed that the whole system here is exposed to the axial magnetic field H_x together with a thermal environment.

2.1. Lorentz force

As mentioned earlier, the existence of a magnetic field in the space results in inducing the corresponding Lorentz force on the structures in that space. It is aimed to present the differential form of Maxwell's equations and then derive the associated Lorentz force from the longitudinal magnetic field. Maxwell's relations for a conducting elastic body are developed as (Narendar, Gupta, & Gopalakrishnan, 2012)

$$J = \nabla \times h, \tag{1}$$

$$\nabla \times E = -\mu \frac{\partial h}{\partial t}, \tag{2}$$

$$\nabla \cdot h = 0, \tag{3}$$

$$E = -\mu \left(\frac{\partial U}{\partial t} \times H \right), \tag{4}$$

$$h = \nabla \times (U \times H) \tag{5}$$

in which U, E, h, and J stand for the displacement vector, the strength vectors of the electric field, the disturbing vectors of the magnetic field, and the current density, respectively. Additionally, $\nabla = \partial/\partial x\, \widehat{\mathbf{e}}_{\mathbf{x}} + \partial/\partial y\, \widehat{\mathbf{e}}_{\mathbf{y}} + \partial/\partial z\, \widehat{\mathbf{e}}_{\mathbf{z}}$ is the Nabla operator and μ denotes the magnetic field permeability. Applying the unidirectional magnetic field $H = (H_x, 0, 0)$ through the longitudinal axis of nanotube and describing the displacement vector of any point in the elastic body by $U = (0, v, w)$, the current density and the disturbing vectors of the magnetic field are written by

$$h = \nabla \times (U \times H) = -H_x \left(\frac{\partial v}{\partial y} + \frac{\partial w}{\partial z} \right) \widehat{\mathbf{e}}_{\mathbf{x}} + H_x \frac{\partial v}{\partial x} \widehat{\mathbf{e}}_{\mathbf{y}} + H_x \frac{\partial w}{\partial x} \widehat{\mathbf{e}}_{\mathbf{z}}, \tag{6}$$

$$J = \nabla \times h = -H_x \left(\frac{\partial^2 v}{\partial x \partial z} - \frac{\partial^2 w}{\partial x \partial y} \right) \widehat{\mathbf{e}}_{\mathbf{x}} - H_x \left(\frac{\partial^2 v}{\partial y \partial z} + \frac{\partial^2 w}{\partial x^2} + \frac{\partial^2 w}{\partial z^2} \right) \widehat{\mathbf{e}}_{\mathbf{y}} + H_x \left(\frac{\partial^2 v}{\partial x^2} + \frac{\partial^2 v}{\partial y^2} + \frac{\partial^2 w}{\partial y \partial z} \right) \widehat{\mathbf{e}}_{\mathbf{z}}. \tag{7}$$

Thereby, the induced Lorentz force, denoted by F_L, which is applied as a body force is given by:

$$F_L = \mu (J \times H) = \mu H_x^2 \left[\left(\frac{\partial^2 v}{\partial x^2} + \frac{\partial^2 v}{\partial y^2} + \frac{\partial^2 w}{\partial y \partial z} \right) \widehat{\mathbf{e}}_{\mathbf{y}} + \left(\frac{\partial^2 w}{\partial x^2} + \frac{\partial^2 w}{\partial y^2} + \frac{\partial^2 v}{\partial y \partial z} \right) \widehat{\mathbf{e}}_{\mathbf{z}} \right]. \tag{8}$$

The only component of the displacement vector is assumed to be the lateral one, i.e. $w = w(x, t)$, and the studied problem is considered as axisymmetric. As a consequence, the z-component of Lorentz force per unit length of the nanotube is given by

$$F_L = F_{zL} \widehat{\mathbf{e}}_{\mathbf{z}} = \mu A H_x^2 \frac{\partial^2 w}{\partial x^2} \widehat{\mathbf{e}}_{\mathbf{z}}, \tag{9}$$

where A stands for the cross-sectional area of the nanotube.

2.2. Continuum nonlocal theory

In the context of Eringen's nonlocal theory of elasticity framework (Eringen, 1972a, 1972b, 1983), it is stated that the field of stress at any point x in an elastic body does not only depend on the field of strain at that point but also on strains at all other neighboring points of the continuum media. Eringen found this conclusion by experimental observations and also an atomic theory. Hence, the nonlocal stress tensor σ_{ij} as a function of the local stress tensor of a continuum domain is defined as

$$\sigma_{ij} = \int_V K\left(|x - x'|, e_0 a\right) t\left(x'\right) dV \tag{10}$$

in which the kernel function $K(|x - x'|, e_0 a)$ represents the modulus of nonlocality, $e_0 a$ shows a material constant depended on external and internal characteristic lengths, $|x - x'|$ denotes the distance (in Euclidean norm) and $t(x)$ is the tensor of local stress at point x. At a point x, the local stress tensor $t(x)$ (assuming a Hookean solid) is related to the strain tensor $\varepsilon(x)$ at the point by the generalized Hooke's law as follows:

$$t(x) = C(x) : \varepsilon(x) \tag{11}$$

in which C illustrates an elasticity tensor with fourth-order (":" represents the "double-dot" (tensor) product operator). To give the nonlocal behavior of a Hookean solid medium, equations (10) and (11) should be considered simultaneously. At a point of an elastic domain, the average of the local strain field to the

stress field over a predefined finite domain is presented by equation (10). A solution for this integral cannot be simply found. But, by assuming the integral ranges from negative infinity to positive one results in a gradient approximation (Eringen, 1972a, 1972b, 1983; Liu & Jeffers, 2019) based on an equivalent differential formulation as

$$t = \sigma - (e_0 a)^2 \nabla^2 \sigma \tag{12}$$

in which a and e_0 are the internal characteristic lengths (e.g. the lattice spacing and wavelength) and material constant (for calibration between the mathematical modeling and empirical data), respectively. The parameter e_0 is vital for the validity of nonlocal models. This parameter can be determined by matching the dispersion curves based on atomistic models.

Based on equations (11) and (12), the components of stress resultant, as a function of the scale factor, can be readily formulated. By applying the operator ∇^2 on the stress resultants in the local domain, the nonlocal theory leads to the differential equations containing the nonlocal stress and strain resultants. Thereby, the nonlocal equilibrium equation is described as follows (Golmakani, Ahmadpour, & Malikan, 2019; Golmakani, Malikan, Sadraee Far, & Majidi, 2018; Malikan & Nguyen, 2018b; Malikan, Jabbarzadeh, & Dastjerdi, 2017; Malikan & Sadraee Far, 2018; Malikan, Tornabene, & Dimitri, 2018):

$$E\varepsilon_{xx} = \sigma_{xx} - (e_0 a)^2 \frac{\partial^2 \sigma_{xx}}{\partial x^2}. \tag{13}$$

In the above equation, the axial strain ε_{xx} is defined by $-z\partial^2 w/\partial x^2$ and thereby the following relationship between the flexural displacement w and the bending moment M of the nanotube can be obtained:

$$-EI\frac{\partial^2 w}{\partial x^2} = M - (e_0 a)^2 \frac{\partial^2 M}{\partial x^2}, \tag{14}$$

where $I = \int_A z^2 dA$ is the second moment of area (inertia) of the nanotube.

2.3. Elastic-beam model with Von-Kármán nonlinearity and thermal effect

EB beam theory is adopted here to efficiently model the nonlinear dynamic behavior of hetero-nanotube. In the case of moderate rotations, the von-Kármán nonlinear strains should be included in the theoretical study. According to the EB elastic beam theory, the nonlinear governing equation of motion takes the following form:

$$\frac{\partial^2 M}{\partial x^2} = m\frac{\partial^2 w}{\partial t^2} - \left(\frac{1}{2}\frac{EA}{L}\int_0^L \left(\frac{\partial w}{\partial x}\right)^2 dx\right)\frac{\partial^2 w}{\partial x^2} - F_{ext}, \tag{15}$$

where M is the resultant bending moment and m is the mass per unit length of the nanotube. Moreover, F_{ext} is the external force in z-direction due to the magnetic field effect that can be written as follows:

$$F_{ext} = F_{zL}. \tag{16}$$

In the context of the thermal elasticity theory framework (Liu & Jeffers, 2018; Liu, Plucinsky, & Jeffers, 2017; Wang, Ni, Li, & Qia, 2008), the temperature gradient in the elastic body leads to the following axial force N_t as

$$N_t = -\frac{EA}{1-2\upsilon}\alpha_x \Delta T, \tag{17}$$

where ΔT stands for the change in temperature, α_x depicts the coefficient of thermal expansion along the nanotube axis, and υ symbolizes the Poisson's ratio of the nanotube. Taking into account the effect of temperature change, the equation of motion governing the nonlinear dynamic behavior of the nanotube is re-formulated as

$$\frac{\partial^2 M}{\partial x^2} = m\frac{\partial^2 w}{\partial t^2} - \left(\frac{1}{2}\frac{EA}{L}\int_0^L \left(\frac{\partial w}{\partial x}\right)^2 dx\right)\frac{\partial^2 w}{\partial x^2} - N_t\frac{\partial^2 w}{\partial x^2} - F_{zL}. \tag{18}$$

The boundary conditions (BCs) for the doubly clamped nanotube are

$$w(0,t) = w(L,t) = \frac{\partial w(0,t)}{\partial x} = \frac{\partial w(L,t)}{\partial x} = 0. \tag{19}$$

2.4. Governing equations of motion

Taking into account the different conditions stated in the previous sections, the nonlinear governing equation of motion for a C/BT hetero-nanotube including the effects of the magnetic field and the nonlocality in the domain will now be developed. By considering the prescribed relations for the external forces and according to equation (18), the dynamic behavior of the nanotube based on the classical EB beam model is governed by

$$\frac{\partial^2 M}{\partial x^2} = m\frac{\partial^2 w}{\partial t^2} - \left(\frac{1}{2}\frac{EA}{L}\int_0^L \left(\frac{\partial w}{\partial x}\right)^2 dx\right)\frac{\partial^2 w}{\partial x^2} + \frac{EA\alpha_x \Delta T}{1-2\upsilon}\frac{\partial^2 w}{\partial x^2} - \mu AH_x^2\frac{\partial^2 w}{\partial x^2}. \tag{20}$$

Assuming the nonlocal elasticity theory and using equation (14) one can achieve the following:

$$EI\frac{\partial^4 w}{\partial x^4} + (m)\frac{\partial^2 w}{\partial t^2} - \left(\frac{1}{2}\frac{EA}{L}\int_0^L \left(\frac{\partial w}{\partial x}\right)^2 dx\right)\frac{\partial^2 w}{\partial x^2} + \frac{EA\alpha_x \Delta T}{1-2\upsilon}\frac{\partial^2 w}{\partial x^2} - \mu AH_x^2\frac{\partial^2 w}{\partial x^2} - (e_0 a)^2\left[(m)\frac{\partial^2 w}{\partial x^2 \partial t^2} - \left(\frac{1}{2}\frac{EA}{L}\int_0^L \left(\frac{\partial w}{\partial x}\right)^2 dx\right)\frac{\partial^4 w}{\partial x^4} + \frac{EA\alpha_x \Delta T}{1-2\upsilon}\frac{\partial^4 w}{\partial x^4} - \mu AH_x^2\frac{\partial^4 w}{\partial x^4}\right] = 0. \tag{21}$$

In this article, it is presumed that the two segments of the structure, i.e. carbon and boron-nitride sections, have similar geometrical parameters and different material properties. Therefore, by assuming equation (21) for two segments of the hetero-nanotube and adding the subscript "C" for carbon and "BN" for boron-nitride, two governing equations can be obtained as

$$E_C I\frac{\partial^4 w}{\partial x^4} + m_C\frac{\partial^2 w}{\partial t^2} - \left(\frac{1}{2}\frac{E_C A}{L}\int_0^L \left(\frac{\partial w}{\partial x}\right)^2 dx\right)\frac{\partial^2 w}{\partial x^2} + \frac{E_C A\alpha_{xC}\Delta T}{1-2\upsilon}\frac{\partial^2 w}{\partial x^2} - \mu AH_x^2\frac{\partial^2 w}{\partial x^2} - (e_0 a)^2\left[m_C\frac{\partial^2 w}{\partial x^2 \partial t^2} - \left(\frac{1}{2}\frac{E_C A}{L}\int_0^L \left(\frac{\partial w}{\partial x}\right)^2 dx\right)\frac{\partial^4 w}{\partial x^4} + \frac{E_C A\alpha_{xC}\Delta T}{1-2\upsilon}\frac{\partial^4 w}{\partial x^4} - \mu AH_x^2\frac{\partial^4 w}{\partial x^4}\right] = 0 \quad \text{for} \quad 0 \le x < \xi L, \tag{22}$$

$$E_{BN} I\frac{\partial^4 w}{\partial x^4} + m_{BN}\frac{\partial^2 w}{\partial t^2} - \left(\frac{1}{2}\frac{E_{BN} A}{L}\int_0^L \left(\frac{\partial w}{\partial x}\right)^2 dx\right)\frac{\partial^2 w}{\partial x^2} + \frac{E_{BN} A\alpha_{xBN}\Delta T}{1-2\upsilon}\frac{\partial^2 w}{\partial x^2} - \mu AH_x^2\frac{\partial^2 w}{\partial x^2} - (e_0 a)^2\left[m_{BN}\frac{\partial^2 w}{\partial x^2 \partial t^2} - \left(\frac{1}{2}\frac{E_{BN} A}{L}\int_0^L \left(\frac{\partial w}{\partial x}\right)^2 dx\right)\frac{\partial^4 w}{\partial x^4}\right.$$

$$+\frac{E_{BN}A\alpha_{xBN}\Delta T}{1-2\upsilon}\frac{\partial^4 w}{\partial x^4}-\mu AH_x^2\frac{\partial^4 w}{\partial x^4}\Bigg]=0 \quad \text{for} \quad \xi L\le x<L. \tag{23}$$

In order to generalize the outcomes of the present study, the following dimensionless parameters are introduced:

$$\bar{x}=\frac{x}{L},\ W=\frac{w}{L},\ \tau=t\sqrt{\frac{E_C I}{m_C L^4}},\ e_n=\frac{e_0 a}{L},\quad \alpha_1=\frac{E_{BN}}{E_C},\quad \alpha_2=\frac{m_{BN}}{m_C},$$
$$\bar{\alpha}_{xC}=\frac{\alpha_{xC}\Delta T}{1-2\upsilon}\frac{L^2}{r^2},\ \bar{\alpha}_{xBN}=\frac{\alpha_{xBN}\Delta T}{1-2\upsilon}\frac{L^2}{r^2},\ h_{3x}=\frac{\mu AH_x^2L^2}{E_C I}, \tag{24}$$

in which r symbolizes the nanotube radius of gyration. By employing the above-mentioned variables, one can obtain:

$$\frac{\partial^4 W_1}{\partial\bar{x}^4}+\frac{\partial^2 W_1}{\partial\tau^2}-\left(\frac{1}{2}\int_0^L\left(\frac{\partial W}{\partial\bar{x}}\right)^2 d\bar{x}\right)\frac{\partial^2 W}{\partial\bar{x}^2}+\bar{\alpha}_{xC}\frac{\partial^2 W_1}{\partial\bar{x}^2}-h_{3x}\frac{\partial^2 W_1}{\partial\bar{x}^2}$$
$$-e_n^2\left[\frac{\partial^4 W_1}{\partial\bar{x}^2\partial\tau^2}-\left(\frac{1}{2}\int_0^L\left(\frac{\partial W}{\partial\bar{x}}\right)^2 d\bar{x}\right)\frac{\partial^4 W}{\partial\bar{x}^4}+\bar{\alpha}_{xC}\frac{\partial^4 W_1}{\partial\bar{x}^4}+-h_{3x}\frac{\partial^4 W_1}{\partial\bar{x}^4}\right]=0,$$
$$\text{for}\quad 0\le\bar{x}<\xi \tag{25}$$

$$\alpha_1\frac{\partial^4 W_2}{\partial\bar{x}^4}+\alpha_2\frac{\partial^2 W_2}{\partial\tau^2}-\left(\frac{\alpha_1}{2}\int_0^L\left(\frac{\partial W}{\partial\bar{x}}\right)^2 d\bar{x}\right)\frac{\partial^2 W}{\partial\bar{x}^2}+\alpha_1\bar{\alpha}_{xBN}\frac{\partial^2 W_2}{\partial\bar{x}^2}-h_{3x}\frac{\partial^2 W_2}{\partial\bar{x}^2}$$
$$-e_n^2\left[\alpha_2\frac{\partial^4 W_2}{\partial\bar{x}^2\partial\tau^2}-\left(\frac{\alpha_1}{2}\int_0^L\left(\frac{\partial W}{\partial\bar{x}}\right)^2 d\bar{x}\right)\frac{\partial^4 W}{\partial\bar{x}^4}+\alpha_1\bar{\alpha}_{xBN}\frac{\partial^4 W_2}{\partial\bar{x}^4}-h_{3x}\frac{\partial^4 W_2}{\partial\bar{x}^4}\right]=0.$$
$$\text{for}\quad \xi\le\bar{x}\le 1 \tag{26}$$

The equations of motion can be simultaneously simulated with the associated boundary/continuity conditions as follows:

$$W_1(0,\tau)=W_2(1,\tau)=\frac{\partial W_1(0,\tau)}{\partial\bar{x}}=\frac{\partial W_2(1,\tau)}{\partial\bar{x}}=0,$$
$$\text{essential } boundary\ conditions \tag{27}$$

$$\left.\begin{aligned}
&W_1(\bar{x},\tau)\big|_{\bar{x}=\xi}=W_2(\bar{x},\tau)\big|_{\bar{x}=\xi}\\
&\left.\frac{\partial W_1(\bar{x},\tau)}{\partial\bar{x}}\right|_{\bar{x}=\xi}=\left.\frac{\partial W_2(\bar{x},\tau)}{\partial\bar{x}}\right|_{\bar{x}=\xi}\\
&\left.\frac{\partial^2 W_1(\bar{x},\tau)}{\partial\bar{x}^2}\right|_{\bar{x}=\xi}=\alpha_1\left.\frac{\partial^2 W_2(\bar{x},\tau)}{\partial\bar{x}^2}\right|_{\bar{x}=\xi}\\
&\left.\frac{\partial^3 W_1(\bar{x},\tau)}{\partial\bar{x}^3}\right|_{\bar{x}=\xi}=\alpha_1\left.\frac{\partial^3 W_2(\bar{x},\tau)}{\partial\bar{x}^3}\right|_{\bar{x}=\xi}
\end{aligned}\right\}\ \begin{matrix}continuity\ conditions\\ at\ the\ junction\ of\ \bar{x}=\xi\end{matrix}. \tag{28}$$

It is worth mentioning that equations (27) and (28) are imposed on the governing equations defined in equations (25) and (26) in the Galerkin-based finite element method.

3. Solution Methodology

As mentioned before, the vibrational governing equation of C-BN hybrid nanotube subjected to the magnetic fluid in a thermal environment given by equations (25) and (26) with the associated boundary/continuity conditions described in equations (27) and (28) can be decomposed using the finite element method. In this study, the elements have two nodes and four degrees of freedom represent the deflection and slope at both ends as follows:

$$d_1^e=W(\bar{x}_e=0),\ d_2^e=\left.\frac{\partial W}{\partial\bar{x}}\right|_{\bar{x}_e=0},\ d_3^e=W(\bar{x}_e=l_e),\ d_4^e=\left.\frac{\partial W}{\partial\bar{x}}\right|_{\bar{x}_e=l_e} \tag{29}$$

in which l_e is the length of 1D element. Since each nanotube element has four degrees of freedom, it is convenient to define the following cubic displacement function for each element as

$$W_e(\bar{x})=a_1+a_2\bar{x}+a_3\bar{x}^2+a_4\bar{x}^3 \tag{30}$$

and thereby the nodal displacements of that element at two end nodes are defined by

$$\{d_e\}^T=[d_1^e\ d_2^e\ d_3^e\ d_4^e] \tag{31}$$

substituting conditions in equation (29) into the displacement function defined by equation (30), yields the following displacement function for each element as

$$W_e(\bar{x})=[N_1\ N_2\ N_3\ N_4]\{d_e\}, \tag{32}$$

where

$$N_1=\frac{2\bar{x}_e^3-3\bar{x}_e^2 l_e+l_e^3}{l_e^3},\quad N_2=\frac{\bar{x}_e^3 l_e-2\bar{x}_e^2 l_e^2+\bar{x}_e l_e^3}{l_e^3},$$
$$N_3=\frac{-2\bar{x}_e^3+3\bar{x}_e^2 l_e}{l_e^3},\quad N_4=\frac{\bar{x}_e^3 l_e-\bar{x}_e^2 l_e^2}{l_e^3}. \tag{33}$$

Assuming the displacement function in equation (32), the Galerkin weighted residuals method (GWRM) with the interpolation function N_i (as the weight function) can then be applied on equations (25) and (26). Moreover, the solution of the considered problem is written by the following form:

$$W_i(\bar{x},\tau)=W_e^i(\bar{x})\exp(\omega\tau),\quad i=1,2 \tag{34}$$

Thereby, by presuming the weak form of the differential equations, the governing equations of motion can be expressed in matrix form given by

$$[M]_e^C\ddot{W}_1+[K]_e^C W_1-N_C[K_{NL}]_e^C W_1=0, \tag{35}$$

$$[M]_e^{BN}\ddot{W}_2+[K]_e^{BN}W_2-N_{BN}[K_{NL}]_e^{BN}W_2=0, \tag{36}$$

where $[K_{NL}]_e^C$ and $[K_{NL}]_e^{BN}$ are the nonlinear stiffness matrices for carbon and boron-nitride segments. The above-mentioned matrices are defined by

$$[M]_e^C=\int_0^{l_e}N^T N\,d\bar{x}+e_n^2\int_0^{l_e}(N')^T N'\,d\bar{x},$$
$$[K]_e^C=\int_0^{l_e}(N'')^T N''\,d\bar{x}-\bar{\alpha}_{xC}\int_0^{l_e}(N')^T N'\,d\bar{x}+h_{3x}\int_0^{l_e}(N')^T N'\,d\bar{x}$$
$$-e_n^2\left[\bar{\alpha}_{xC}\int_0^{l_e}(N'')^T N''\,d\bar{x}-h_{3x}\int_0^{l_e}(N'')^T N''\,d\bar{x}\right],$$
$$[K_{NL}]_e^C=\int_0^{l_e}(N')^T N'\,d\bar{x}, \tag{37}$$

$$[M]_e^{BN}=\alpha_2\int_0^{l_e}N^T N\,d\bar{x}+e_n^2\alpha_2\int_0^{l_e}(N')^T N'\,d\bar{x},$$
$$[K]_e^{BN}=\alpha_1\int_0^{l_e}(N'')^T N''\,d\bar{x}-\alpha_1\bar{\alpha}_{xBN}\int_0^{l_e}(N')^T N'\,d\bar{x}+h_{3x}\int_0^{l_e}(N')^T N'\,d\bar{x}$$
$$-e_n^2\left[\alpha_1\bar{\alpha}_{xBN}\int_0^{l_e}(N'')^T N''\,d\bar{x}-h_{3x}\int_0^{l_e}(N'')^T N''\,d\bar{x}\right],$$
$$[K_{NL}]_e^{BN}=\int_0^{l_e}(N')^T N'\,d\bar{x} \tag{38}$$

in which the matrices $[K]$ and $[M]$ represent stiffness and

Table 1: Properties of CNT and BNNT sections of hybrid nanotube.

Properties	CNT	BNNT
Young's modulus (E) (TPa) (Cheng et al., 2019)	1	1.8
Density (ρ) (g/cm^3)	2.3	2.18
Outer radius (nm)	3.5	3.5
Aspect ratio ($L/2R_{out}$)	100	100
Thickness (h) (nm)	0.34	0.34
Coefficient of thermal expansion (room temperature) (K^{-1})	-1.6×10^{-6}	-0.3×10^{-6}
Coefficient of thermal expansion (high temperature) (K^{-1})	1.1×10^{-6}	0.2×10^{-6}

Table 2: Comparison of the nonlinear natural frequencies of clamped–clamped homogeneous beam with different initial displacement W_{max}.

	$(\omega_{NL}/\omega_L)^2$			
W_{max}/r	GFEM[a] (Bhashyam & Prathap, 1980)	RGFEM[b] (Bhashyam & Prathap, 1980)	ASM[c] (Evensen, 1968)	Present analysis
0.1	1.0006	1.0006	1.0006	1.0006
0.2	1.0024	1.0024	1.0024	1.0024
0.4	1.0096	1.0096	1.0096	1.0096
0.6	1.0216	1.0216	1.0216	1.0216
0.8	1.0383	1.0384	1.0384	1.0383
1	1.0598	1.0599	1.0600	1.0598
1.5	1.1343	1.1349	1.1349	1.1343
2	1.2381	1.2398	1.2398	1.2382
3	1.5319	1.5395	1.5396	1.5320
4	1.9376	1.9591	1.9592	1.9377
5	2.4520	2.4986	2.4988	2.4522

r = radius of gyration; W_{max} = maximum initial amplitude.
[a]Generalized finite element method (GFEM).
[b]Reduced GFEM (RGFEM).
[c]Assumed space mode (ASM).

mass coefficients, respectively. After applying the boundary/continuity conditions, using the assumed solution and performing the usual assemblage process, the characteristic equation for the hybrid C/BN nanotube is extracted as

$$\left(\omega^2 [M] + [K] + N [K_{NL}]\right) \{\Delta_e\} = 0, \tag{39}$$

where ω and Δ_e are the eigenvalue and eigenvector of the problem. Moreover, the non-dimensional nonlinear force N can be computed as the summation of the axial forces for two segments given by

$$N = N_C + N_{BN} = \frac{1}{2}\sum_{i=1}^{n_C}\int_0^{l_e} W_{1,\bar{x}}^2 \, d\bar{x} + \frac{\alpha_1}{2}\sum_{i=1}^{n_{BN}}\int_0^{l_e} W_{2,\bar{x}}^2 \, d\bar{x}$$

$$= \frac{1}{2}\{\Delta_e\}^T [K_{NL}]^C \{\Delta_e\} + \frac{\alpha_1}{2}\{\Delta_e\}^T [K_{NL}]^{BN} \{\Delta_e\}. \tag{40}$$

In order to solve the nonlinear eigenvalue problem described in equation (39), one can try to compute the exact nonlinear mode shape and the value of nonlinear frequency ω_{NL} corresponding to this mode can then be calculated. First, the initial amplitude of vibration is selected – here we assume that the initial amplitude of the hybrid nanotube is the first mode shape of the linear system. Then the linear mode shape should be normalized to attain the maximum desired amplitude W_{max}. Thereby, the nonlinear stiffness matrix for the whole nanotube $[K_{NL}]$ is calculated. The linearized eigenvalue problem (39) leads to a modified nonlinear mode shape Δ_e as well as the corresponding nonlinear frequency ω_{NL}. The obtained mode shape should be normalized to get the desired maximum amplitude of the hybrid nanotube and this strategy is repeated until the selected convergence criterion is satisfied.

4. Results and Discussion

In this section, at first, some comparative studies are performed with the results of published works in the literature to verify the soundness of the present analysis. Then, the nonlinear vibrational characteristics of hetero-nanotube are exhibited by conducting some numerical examples and studying the variations of the natural frequencies and mode shapes of C/BN nanotube.

4.1. Integrity of present analysis

To justify the integrity of our analysis, the following material and geometrical properties for carbon and boron-nitride sections are used in the simulations (see Table 1).

Since there is no research work on the nonlinear vibration analysis of a doubly-clamped C/BN nanotube in the magnetic/thermal environment, in order to validate the results of the current study, the natural frequencies of a homogenous beam in comparison with the results obtained in the literature are tabulated in Table 2. The comparison of the numerical values presented in Table 2 shows the excellent agreement between our analysis and those reported in Bhashyam and Prathap (1980) and Evensen (1968). Although the obtained results are getting gradually far from the references after $W_{max}/r = 2$, their diversity is insignificant and originates from different numerical

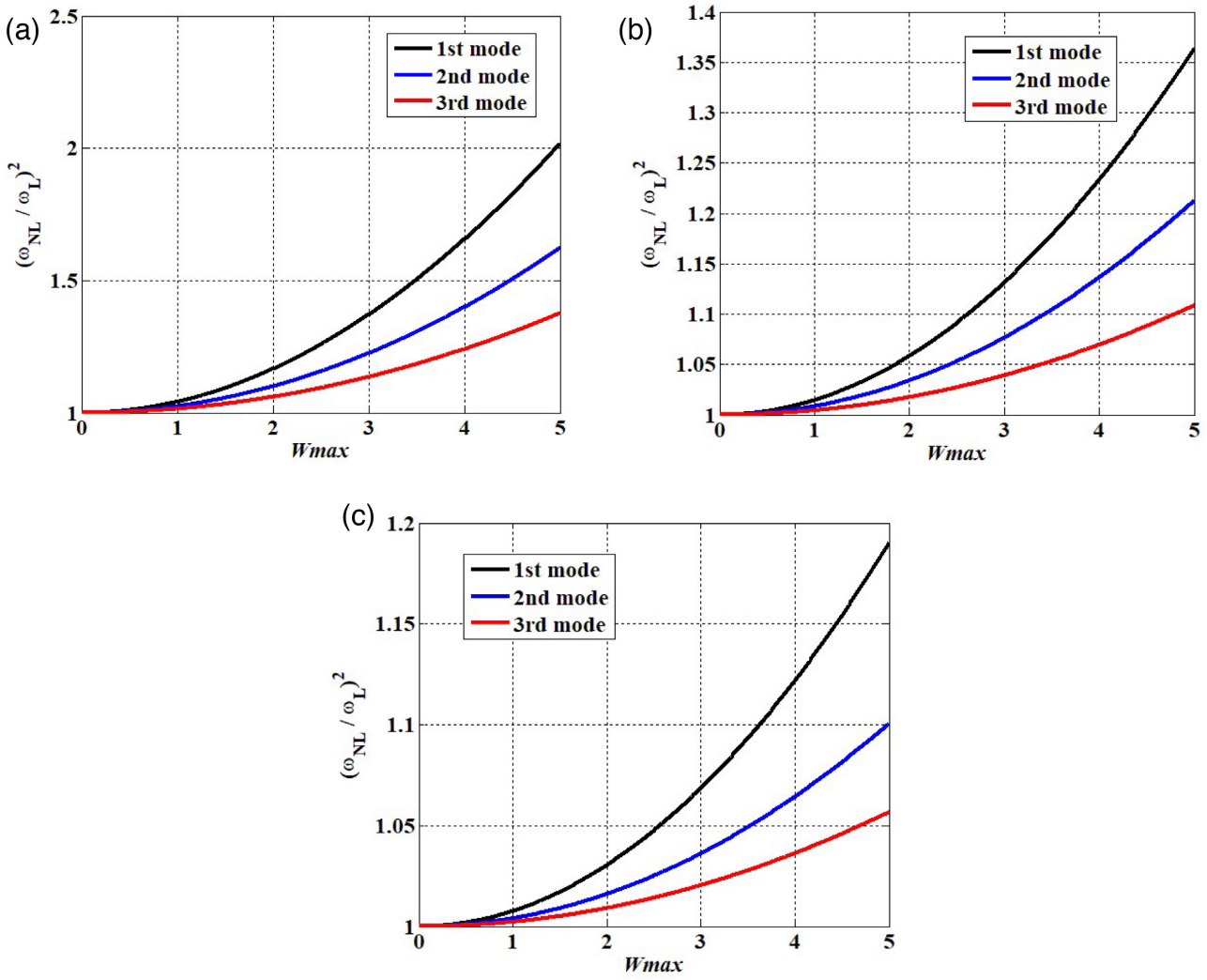

Figure 2: Dimensionless frequency ratio (ω_{NL}/ω_L) vs. the maximum deflection for (a) $h_{3x} = 0.5$, $\Delta T = 200$, room temperature, $\xi = 0.3$, and $e_n = 0$; (b) $h_{3x} = 0.5$, $\Delta T = 200$, room temperature, $\xi = 0.3$, and $e_n = 0.5$; and (c) $h_{3x} = 0.5$, $\Delta T = 200$, room temperature, $\xi = 0.8$, and $e_n = 0.5$.

algorithms. It is clearly obvious that the results computed by the present analysis tend to be closer to the GFEM results.

4.2. Numerical analysis

In this section, the nonlinear vibration analysis of hybrid nanotube made of carbon and boron-nitride segments is investigated through plotting the variations of the first three natural frequencies and mode shapes of the nanostructure. To this end, Fig. 2a–c presents the ratio of nonlinear to linear frequencies of the system vs. the maximum initial deflection of the nanotube. It is obvious that as initial deflection increases, the ratio of nonlinear to linear frequencies is remarkably increased that demonstrates the significant influence of the amplitude of vibration on the nonlinear natural frequencies. According to the plotted curves in Fig 2a, for the classical nanotube, the first nonlinear frequency is more sensitive to the initial condition of the nanotube denoted by W_{max}. In other words, the variations of the first nonlinear frequency are more than the second and third one for specific values of W_{max}. It is clearly demonstrated that the hetero-nanotube exhibits hardening behavior with respect to the initial deflection. In the second part of this figure, Fig. 2b, the effect of nonlocality of the nanotube is taken into account. It is important to find that the frequency ratio (ω_{NL}/ω_L) is dropped in the case of the nonlocal theory compared to the classical one. For a more in-depth investigation, Fig. 2c is presented, in which ξ takes the value of 0.8 and the other parameters remain constant compared to Fig. 2b. In Fig. 2b, the hybrid nanotube had 30% of the CNT length, and in Fig. 2c its percentage is 80%. It is revealed that the difference between the values of the first and second modes slightly increase. On the other hand, one can conclude that by increasing the contribution of the CNT in hetero-nanotube the values of the frequency ratio will decrease for the first natural frequencies.

Figure 3a–g depicts different configurations of the first three nonlinear modes of the hybrid nanotube in different conditions. In the first and second diagrams, the homogenous CNT and the hybrid nanotube with $\xi = 0.3$ are illustrated in the context of the classical beam framework and in Fig. 3c, the hybrid nanotube with $\xi = 0.3$ is plotted with the same parameters as the second figure, but for the case of a nonlocal model with $e_n = 0.5$. In Fig. 3d, a larger value for the nonlocal parameter $e_n = 1$ is assumed. It is important to note that for the local beam model of a

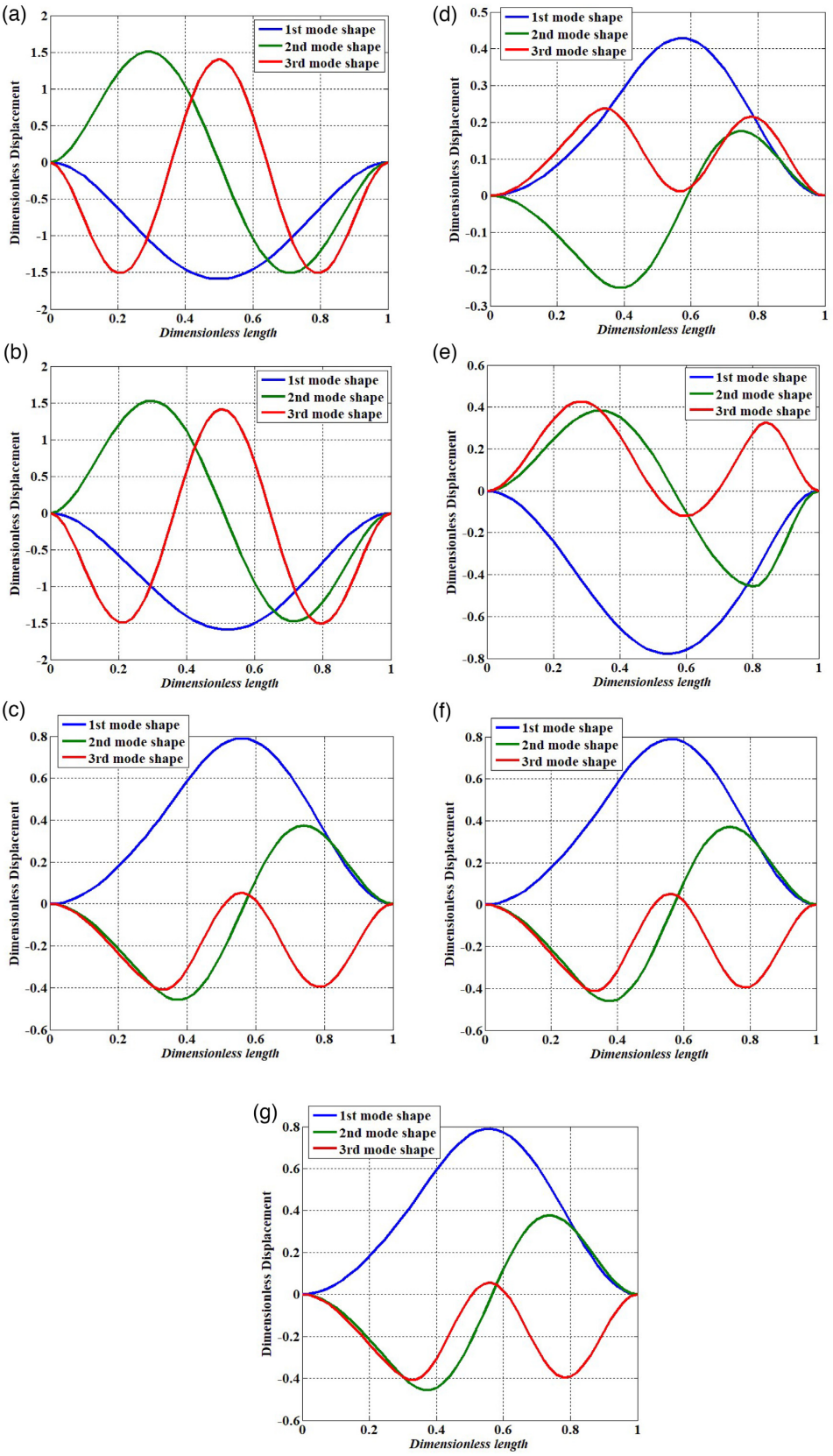

Figure 3: Dimensionless displacement vs. dimensionless length of a CNT in several nonlinear vibrational modes for (a) $h_{3x} = 0.5$, $W_{max}/r = 5$, $\Delta T = 0$, room temperature, $\xi = 1$, $e_n = 0$; (b) $h_{3x} = 0.5$, $W_{max}/r = 5$, $\Delta T = 200$, room temperature, $\xi = 0.3$, $e_n = 0$; (c) $h_{3x} = 0.5$, $W_{max}/r = 5$, $\Delta T = 200$, room temperature, $\xi = 0.3$, $e_n = 0.5$; (d) $h_{3x} = 0.5$, $W_{max}/r = 5$, $\Delta T = 200$, room temperature, $\xi = 0.3$, $e_n = 1$; (e) $h_{3x} = 0.5$, $W_{max}/r = 5$, $\Delta T = 200$, room temperature, $\xi = 0.8$, $e_n = 0.5$; (f) $h_{3x} = 0$, $W_{max}/r = 5$, $\Delta T = 200$, room temperature, $\xi = 0.3$, $e_n = 0.5$; and (g) $h_{3x} = 1$, $W_{max}/r = 5$, $\Delta T = 200$, room temperature, $\xi = 0.3$, $e_n = 0.5$.

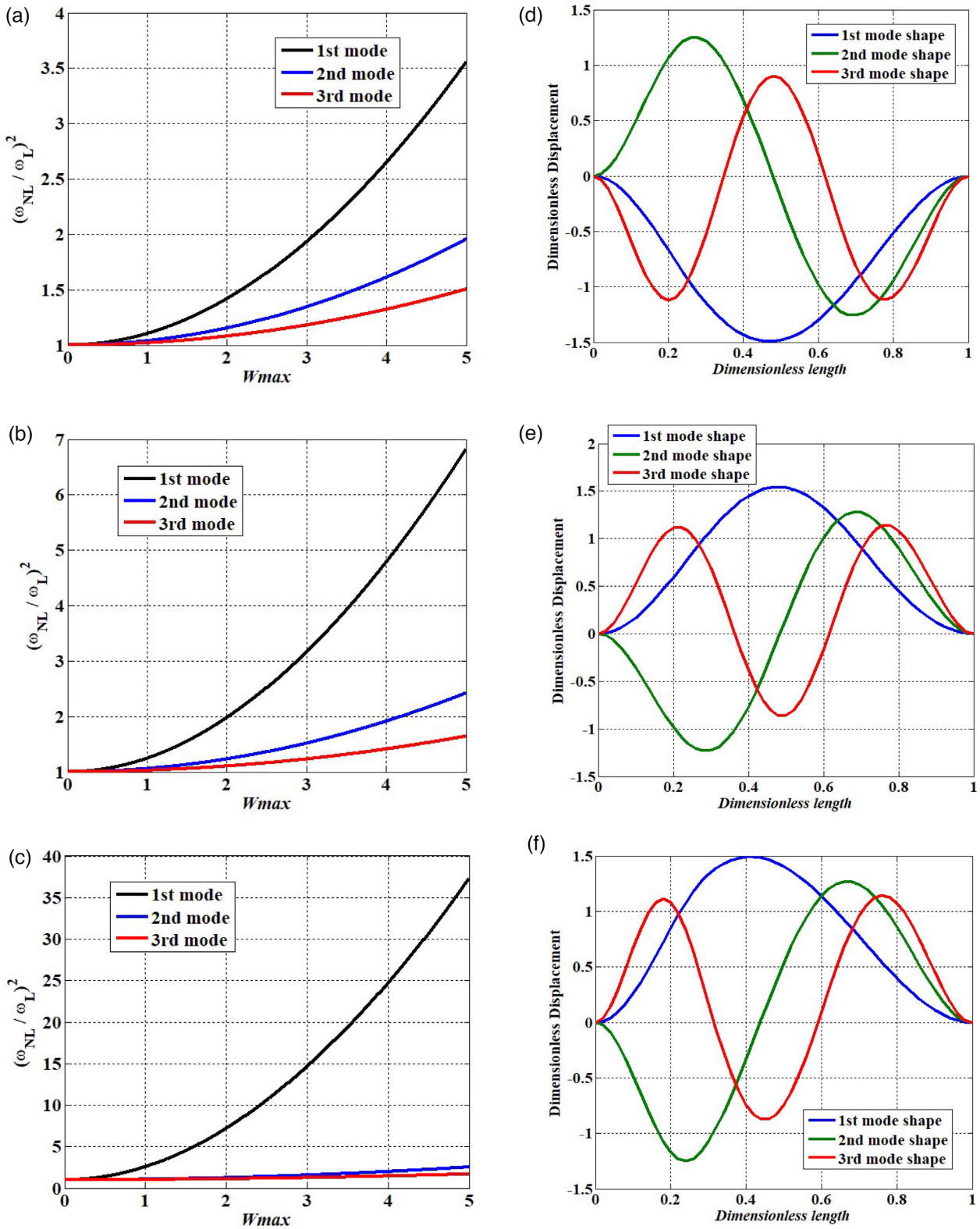

Figure 4: (a) Dimensionless frequency ratio (ω_{NL}/ω_L) vs. the maximum deflection for $h_{3x} = 0.1$, $\Delta T = 200$, high temperature, $\xi = 0.3$, $e_n = 0.1$). (b) Dimensionless frequency ratio (ω_{NL}/ω_L) vs. the maximum deflection for $h_{3x} = 0.1$, $\Delta T = 200$, high temperature, $\xi = 0.8$, $e_n = 0.1$. (c) Dimensionless frequency ratio (ω_{NL}/ω_L) vs. the maximum deflection for $h_{3x} = 0.1$, $\Delta T = 400$, high temperature, $\xi = 0.3$, $e_n = 0.1$. (d) Dimensionless displacement vs. dimensionless length of a CNT in several nonlinear vibrational modes for $h_{3x} = 0.1$, $W_{max}/r = 5$, $\Delta T = 200$, high temperature, $\xi = 0.3$, $e_n = 0.1$. (e) Dimensionless displacement vs. dimensionless length of a CNT in several nonlinear vibrational modes for $h_{3x} = 0.1$, $W_{max}/r = 5$, $\Delta T = 200$, high temperature, $\xi = 0.8$, $e_n = 0.1$. (f) Dimensionless displacement vs. dimensionless length of a CNT in several nonlinear vibrational modes for $h_{3x} = 0.1$, $W_{max}/r = 5$, $\Delta T = 400$, high temperature, $\xi = 0.3$, $e_n = 0.1$.

homogeneous nanotube (Fig. 3a) and in the first mode, the maximum deflection occurs at the center of the nanotube, however, as illustrated in Fig. 3b, the position of the maximum deflection is slightly deviated from the center of the nanotube because of the difference between the modulus of elasticity of the two segments. Moreover, in the nonlocal analysis and in the first mode, the maximum deflection does not occur at the nanotube center and the deviation is also significant for the second and third modes of the third graph compared to the second one. For example, in the third mode of the nonlocal analysis, the maximum deflection does not take place in the center of the nanotube, whereas for the classical beam theory the maximum deflection is located at the center of the nanotube. By comparing the third mode configurations for the classical and nonlocal analysis, it is also worth mentioning that the third mode shape in the nonlocal theory is quite different compared to the results obtained from the classical beam theory. This means that taking into account the influence of nonlocal elasticity has an evident effect on the configuration of the mode shapes of the hetero-nanotube.

In order to better understand the effect of nonlocality, in Fig. 3d, a higher value of the nonlocal parameter is considered. As it can be seen, the shape of the modes does not significantly change against the previous one in the first and second modes, however, it has a meaningful effect of the configuration of the third mode. It is obviously inferred that the greater values of the nonlocal parameter have much more influence on the higher mode shapes of the nanotube. Moreover, Fig. 3e is plotted by considering the same parameters as in Fig. 3c but with a difference in the value of the length ratio ξ. By comparing Fig. 3c and e, one concludes that the configuration of the mode shapes, especially in the case of the second and third one, might be remarkably changed. In fact, it can be stated that the variation of length ratio ξ may fundamentally alter the vibrational modes of the hetero-nanotube in comparison with the homogenous one.

Finally, in Fig. 3f and g, the effect of magnetic field on the vibrational modes of the system are investigated. It is observed that the shapes of the vibrational modes do not appreciably change and therefore the magnetic field has no meaningful effect on the configuration of nonlinear mode shapes.

Figure 4a–f presents the influence of high-temperature environment on the nonlinear natural frequencies as well as the mode shapes of hetero-nanotubes. In Fig. 4a and b, the selected parameters have the same values except for the length ratio that is $\xi = 0.3$ for the first diagram and $\xi = 0.8$ for the second one. It can be clearly seen how the length ratio would affect the frequency ratio (ω_{NL}/ω_L) of the hybrid nanotubes and in particular how significantly it would increase the nonlinear to linear frequency ratio of the first mode. Additionally, it is evident that the frequency ratio shifts upward by increasing the contribution of carbon segment in the hetero-nanotube. On the other hand, Fig. 4c depicts the impact of the higher temperature change on the variation of the nonlinear natural frequencies. According to the obtained results, it is concluded that the higher temperature gradient dramatically increases the natural frequencies of the system, especially for the first vibrational mode. Moreover, it can be deduced that the nonlinear frequency of the hetero-nanotube is more sensitive to the variation of the initial amplitudes in a high-temperature environment. The current discussion can be supplemented by further examinations based on the results of Fig. 4d–f. As can be seen, the location of the maximum amplitude will move to the left by considering higher temperature gradients when the contribution of the boron-nitride section is dominant.

5. Conclusions

The simultaneous effects of the length ratio, size dependency, magnetic field, and thermal environment on the nonlinear vibrational characteristics of a composite CNT/BNNT were elucidated. The governing equations were derived within the context of the EB beam theory framework in the presence of Eringen's nonlocal elasticity. The numerical results were extracted by assuming the initial deflection similar to the first mode shape of the linear problem. A nonlinear finite element formulation was applied to discretize the governing differential equations. According to the findings of this study, it is concluded that

1. the initial amplitude increases the nonlinear natural frequencies of the nanotube, and especially in the case of the fundamental frequency, its effect is much more meaningful;
2. the vibrational mode shapes might be very different when the nonlocal parameter is included in the simulations. As a result, the nonlocal analysis will lead to a deviation in the location of maximum deflections;
3. high-temperature environment strongly affects the configuration of the nonlinear mode shapes;
4. the location of the maximum amplitude will move to the left by considering higher temperature gradients when the contribution of the boron-nitride section is dominant.

Acknowledgement

The authors would like to take this opportunity to express their appreciation to Mr Ali Heydari Shirazi for his efforts on providing 3D configuration of the studied structure shown in Fig. 1.

Conflict of interest statement

Declarations of interest: none.

References

Agwa, M. A., & Eltaher, M. A. (2016). Vibration of a carbyne nanomechanical mass sensor with surface effect. *Applied Physics A*, *122*, 335.

Ansari, R., Gholami, R., & Ajori, S. (2013). Torsional vibration analysis of carbon nanotubes based on the strain gradient theory and molecular dynamic simulations. *Journal of Vibration and Acoustics*, *135*, 051016.

Badjian, H., & Setoodeh, A. R. (2017). Improved tensile and buckling behavior of defected carbon nanotubes utilizing boron nitride coating – A molecular dynamics study. *Physica B: Condensed Matter*, *507*, 156–163.

Barretta, R., Čanadija, M., & Marotti de Sciarra, F. (2016). A higher-order Eringen model for Bernoulli–Euler nanobeams. *Archive of Applied Mechanics*, *86*, 483–495.

Barretta, R., Čanadija, M., & Marotti de Sciarra, F. (2019). Modified nonlocal strain gradient elasticity for nano-rods and application to carbon nanotubes. *Applied Sciences (Switzerland)*, *9*(3), Article number 514.

Barretta, R., Faghidian, S. A., Marotti de Sciarra, F., & Pinnola, F. P. (2019). Timoshenko nonlocal strain gradient nanobeams: Variational consistency, exact solutions and carbon nanotube Young moduli. *Mechanics of Advanced Materials and Structures*. DOI:10.1080/15376494.2019.1683660.

Barretta, R., & Marotti de Sciarra, F. (2019). Variational nonlocal gradient elasticity for nano-beams. *International Journal of Engineering Science*, *143*, 73–91.

Bhashyam, G. R., & Prathap, G. (1980). Galerkin finite element method for nonlinear beam vibrations. *Journal of Sound and Vibration*, *72*, 191–203.

Chang, T.-P. (2017). Nonlinear vibration of single-walled carbon nanotubes with nonlinear damping and random material properties under magnetic field. *Composites Part B: Engineering*, *114*, 69–79.

Chen, X. K., Xie, Z. X., Zhang, Y., Deng, Y. X., Zou, T. H., Liu, J., & Chen, K. Q. (2019). Highly efficient thermal rectification in carbon/boron nitride heteronanotubes. *Carbon*, *148*, 532–539.

Cheng, Q., Liu, Y. S., Wang, G. C., Liu, H., Jin, M. G., & Li, R. (2019). Free vibration of a fluid-conveying nanotube constructed by carbon nanotube and boron nitride nanotube. *Physica E: Low-dimensional Systems and Nanostructures*, *109*, 183–190.

Choyal, V. K., Choyal, V., Nevhal, S., Bergaley, A., & Kundalwal, S. I. (2019). Effect of aspects ratio on Young's modulus of boron nitride nanotubes: A molecular dynamics study. *Materials Today Proceedings*. https://doi.org/10.1016/j.matpr.2019.05.347.

Eltaher, M. A., Abdraboh, A. M., & Almitani, K. H., (2018). Resonance frequencies of size dependent perforated nonlocal nanobeam. *Microsystem Technologies*, *24*, 3925–3937.

Eltaher, M. A., & Agwa, M. A. (2016). Analysis of size-dependent mechanical properties of CNTs mass sensor using energy equivalent model. *Sensors and Actuators A: Physical*, *246*, 9–17.

Eltaher, M. A., Almalki, T. A., Ahmed, K. I. E., & Almitani, K. H. (2019). Characterization and behaviors of single walled carbon nanotube by equivalent-continuum mechanics approach. *Advances in Nano Research*, *7*, 39–49.

Eltaher, M. A., Almalki, T. A., Almitani, K. H., & Ahmed, K. I. E. (2019). Participation factor and vibration of carbon nanotube with vacancies. *Journal of Nano Research*, *57*, 158–174.

Eltaher, M. A., Almalki, T. A., Almitani, K. H., Ahmed, K. I. E., & Abdraboh, A. M. (2019). Modal participation of fixed–fixed single-walled carbon nanotube with vacancies. *International Journal of Advanced Structural Engineering*, *11*, 151–163.

Eltaher, M. A., El-Borgi, S., & Reddy, J. N. (2016). Nonlinear analysis of size-dependent and material-dependent nonlocal CNTs. *Composite Structures*, *153*, 902–913.

Eltaher, M. A., Khater, M. E., Abdel-Rahman, E., & Yavuz, M. (2014). Model for nano-scale bonding wires under thermal loading. In *14th IEEE international conference on nanotechnology* (pp. 382–385), Toronto, ON, Canada.

Eltaher, M. A., Khater, M. E., & Emam, S. A. (2016). A review on nonlocal elastic models for bending, buckling, vibrations, and wave propagation of nanoscale beams. *Applied Mathematical Modelling*, *40*, 4109–4128.

Eltaher, M. A., Mohamed, N., Mohamed, S. A., & Seddek, L. F. (2019). Postbuckling of curved carbon nanotubes using energy equivalent model. *Journal of Nano Research*, *57*, 136–157.

Eltaher, M. A., Omar, F. A., Abdalla, W. S., & Gad, E. H. (2019). Bending and vibrational behaviors of piezoelectric nonlocal nanobeam including surface elasticity. *Waves in Random and Complex Media*, *29*, 264–280.

Emam, S. A., Eltaher, M. A., Khater, M. E., & Abdalla, W. S. (2018). Postbuckling and free vibration of multilayer imperfect nanobeams under a pre-stress load. *Applied Sciences*, *8*, 2238.

Eringen, A. C. (1972a). Linear theory of nonlocal elasticity and dispersion of plane waves. *International Journal of Engineering Science*, *10*, 425–435.

Eringen, A. C. (1972b). Nonlocal polar elastic continua. *International Journal of Engineering Science*, *10*, 1–16.

Eringen, A. C. (1983). On differential equations of nonlocal elasticity and solutions of screw dislocation and surface waves. *Journal of Applied Physics*, *54*, 4703–4710.

Evensen, D. A. (1968). Nonlinear vibrations of beams with various boundary conditions. *American Institute of Aeronautics and Astronautics Journal*, *6*, 370–372.

Genoese, A. L., Genoese, A. N., & Salerno, G. (2019). On the nanoscale behaviour of single-wall C, BN and SiC nanotubes. *Acta Mechanica*, *230*, 1105–1128. https://doi.org/10.1007/s00707-018-2336-7.

Ghalambaz, M., Ghalambaz, M., & Edalatifar, M. (2015). Buckling analysis of cantilever nanoactuators immersed in an electrolyte: A close form solution using Duan–Rach modified adomian decomposition method. *Journal of Applied and Computational Mechanics*, *1*, 207–219.

Ghalambaz, M., Ghalambaz, M., & Edalatifar, M. (2016). A new analytic solution for buckling of doubly clamped nanoactuators with integro differential governing equation using Duan–Rach adomian decomposition method. *Applied Mathematical Modelling*, *40*, 7293–7302.

Golmakani, M. E., Ahmadpour, M., & Malikan, M. (2019). Thermal buckling analysis of circular bilayer graphene sheets resting on an elastic matrix based on nonlocal continuum mechanics. *Journal of Applied and Computational Mechanics*. DOI:10.22055/JACM.2019.31299.1859.

Golmakani, M. E., Malikan, M., Sadraee Far, M. N., & Majidi, H. R. (2018). Bending and buckling formulation of graphene sheets based on nonlocal simple first order shear deformation theory. *Materials Research Express*, *5*, 065010.

Hamed, M. A., Sadoun, A. M., & Eltaher, M. A. (2019). Effects of porosity models on static behavior of size dependent functionally graded beam. *Structural Engineering and Mechanics*, *71*, 89–98.

Jena, S. K., Chakraverty, S., & Malikan, M. (2019). Implementation of Haar wavelet, higher order Haar wavelet, and differential quadrature methods on buckling response of strain gradient nonlocal beam embedded in an elastic medium. *Engineering with Computers*.https://doi.org/10.1007/s00366-019-00883-1.

Jena, S. K., Chakraverty, S., Malikan, M., & Tornabene, F. (2019). Stability analysis of single-walled carbon nanotubes embedded in winkler foundation placed in a thermal environment considering the surface effect using a new refined beam theory. *Mechanics Based Design of Structures and Machines, An International Journal*. https://doi.org/10.1080/15397734.2019.1698437

Liu, N., & Jeffers, A. E. (2018). Adaptive isogeometric analysis in structural frames using a layer-based discretization to model spread of plasticity. *Computers & Structures*, *196*, 1–11.

Liu, N., & Jeffers, A. E. (2019). Feature-preserving rational Bézier triangles for isogeometric analysis of higher-order gradient damage models. *Computer Methods in Applied Mechanics and Engineering*, *357*, 112585.

Liu, N., Plucinsky, P., & Jeffers, A. E. (2017). Combining load-controlled and displacement-controlled algorithms to model thermal-mechanical snap-through instabilities in structures. *Journal of Engineering Mechanics*, 143. https://doi.org/10.1061/(ASCE)EM.1943-7889.0001263.

Malikan, M. (2017). Electro-mechanical shear buckling of piezoelectric nanoplate using modified couple stress theory based on simplified first order shear deformation theory. *Applied Mathematical Modelling*, *48*, 196–207.

Malikan, M. (2018). Temperature influences on shear stability of a nanosize plate with piezoelectricity effect. *Multidiscipline Modeling in Materials and Structures*, *14*, 125–142.

Malikan, M. (2019a). Electro-thermal buckling of elastically supported double-layered piezoelectric nanoplates affected by an external electric voltage. *Multidiscipline Modeling in Materials and Structures*, *15*, 50–78.

Malikan, M. (2019b). On the buckling response of axially pressurized nanotubes based on a novel nonlocal beam theory. *Journal of Applied and Computational Mechanics*, 5,103–112.

Malikan, M., Dimitri, R., & Tornabene, F. (2019). Transient response of oscillated carbon nanotubes with an internal and external damping. *Composites Part B: Engineering*, *158*, 198–205.

Malikan, M., Jabbarzadeh, M., & Dastjerdi, Sh. (2017). Non-linear static stability of bi-layer carbon nanosheets resting on an elastic matrix under various types of in-plane shearing loads in thermo-elasticity using nonlocal continuum. *Microsystem Technologies*, *23*, 2973–2991.

Malikan, M., & Nguyen, V. B. (2018a). A novel one-variable first-order shear deformation theory for biaxial buckling of a size-dependent plate based on the Eringen's nonlocal differential law. *World Journal of Engineering*, *15*, 633–645.

Malikan, M., & Nguyen, V. B. (2018b). Buckling analysis of piezo-magnetoelectric nanoplates in hygrothermal environment based on a novel one variable plate theory combining with higher-order nonlocal strain gradient theory. *Physica E: Low-dimensional Systems and Nanostructures*, *102*, 8–28.

Malikan, M., Nguyen, V. B., Dimitri, R., & Tornabene, F. (2019). Dynamic modeling of non-cylindrical curved viscoelastic single-walled carbon nanotubes based on the second gradient theory. *Materials Research Express*, *6*, 075041.

Malikan, M., Nguyen, V. B., & Tornabene, F. (2018a). Electromagnetic forced vibrations of composite nanoplates using nonlocal strain gradient theory. *Materials Research Express*, *5*, 075031.

Malikan, M., Nguyen, V. B., & Tornabene, F. (2018b). Damped forced vibration analysis of single-walled carbon nanotubes resting on viscoelastic foundation in thermal environment using nonlocal strain gradient theory. *Engineering Science and Technology, An International Journal*, *21*, 778–786.

Malikan, M., & Sadraee Far, M. N. (2018). Differential quadrature method for dynamic buckling of graphene sheet coupled by a viscoelastic medium using neperian frequency based on nonlocal elasticity theory. *Journal of Applied and Computational Mechanics*, 4, 147–160.

Malikan, M., Tornabene, F., & Dimitri, R. (2018). Nonlocal three-dimensional theory of elasticity for buckling behavior of functionally graded porous nanoplates using volume integrals. *Materials Research Express*, *5*, 095006.

Mohamed, N., Eltaher, M. A., Mohamed, S. A., & Seddek, L. F. (2019). Energy equivalent model in analysis of postbuckling of imperfect carbon nanotubes resting on nonlinear elastic foundation. *Structural Engineering and Mechanics*, *70*, 737–750.

Narendar, S., Gupta, S. S., & Gopalakrishnan, S. (2012). Wave propagation in single-walled carbon nanotube under longitudinal magnetic field using nonlocal Euler–Bernoulli beam theory. *Applied Mathematical Modelling*, *36*, 4529–4538.

Noghrehabadi, A. R., Eslami, M., & Ghalambaz, A. (2013). Influence of size effect and elastic boundary condition on the pull-in instability of nano-scale cantilever beams immersed in liquid electrolytes. *International Journal of Non-Linear Mechanics*, *52*, 73–84.

Noghrehabadi, A. R., Ghalambaz, M., & Ghanbarzadeh, A. (2012). A new approach to the electrostatic pull-in instability of nanocantilever actuators using the ADM–Padé technique. *Computers & Mathematics with Applications*, *64*, 2806–2815.

Nozaki, H., & Itho, S. (1996). Lattice dynamics of a layered material BC2N. *Physica B: Condensed Matter*, *219–220*, 487–489.

Ouakad, H. M., & Sedighi, H. M. (2016). Rippling effect on the structural response of electrostatically actuated single-walled carbon nanotube based NEMS actuators. *International Journal of Non-Linear Mechanics*, *87*, 97–108.

Ramezannejad Azarboni, H. (2019). Magneto-thermal primary frequency response analysis of carbon nanotube considering surface effect under different boundary conditions. *Composites Part B: Engineering*, *165*, 435–441.

Rodríguez Juárez, A. R., Anota, E. C., Cocoletzi, H. H., Sánchez Ramírez, J. F., & Castro, M. (2017). Stability and electronic properties of armchair boron nitride/carbon nanotubes. *Fullerenes, Nanotubes and Carbon Nanostructures*, *25*(12), 716–725.

Sedighi, H. M. (2014). Size-dependent dynamic pull-in instability of vibrating electrically actuated microbeams based on the strain gradient elasticity theory. *Acta Astronautica*, *95*(1), 111–123.

Sedighi, H. M., & Bozorgmehri, A. (2016). Dynamic instability analysis of doubly clamped cylindrical nanowires in the presence of Casimir attraction and surface effects using modified couple stress theory. *Acta Mechanica*, *227*(6), 1575–1591.

Stephan, O., Ajayan, P. M., Colliex, C., Redlich, P., Lambert, J. M., Bernier, P., & Lefin, P. (1994). Doping graphitic and carbon nanotube structures with boron and nitrogen. *Science*, *266*, 1683–1685.

Vedaei, S. S., & Nadimi, E. (2019). Gas sensing properties of CNT-BNNT-CNT nanostructures: A first principles study. *Applied Surface Science*, *470*, 933–942.

Wang, L., Ni, Q., Li, M., & Qia, Q. (2008). The thermal effect on vibration and instability of carbon nanotubes conveying fluid. *Physica E*, *40*, 3179–3182.

Xiao, H., Zhang, C. X., Zhang, K. W., Sun, L. Z., & Zhong, J. X. (2013). Tunable differential conductance of single wall C/BN nanotube heterostructure. *Journal of Molecular Modeling*, *19*, 2965–2969.

Yazdanpanahi, E., Noghrehabadi, A. R., & Ghalambaz, A. (2014). Effect of dielectric-layer on the stress field of micro cantilever beams at the onset of pull-in instability. *Journal of Mechanics*, *30*, 49–56.

Yazdanpanahi, E., Noghrehabadi, A. R., & Ghanbarzadeh, A. (2013). Balance dielectric layer for micro electrostatic switches in the presence of capillary effect. *International Journal of Mechanical Sciences*, *74*, 83–90.

Zhang, J., & Wang, C. Y. (2017). Beat vibration of hybrid boron nitride-carbon nanotubes – A new avenue to atomic-scale mass sensing. *Computational Materials Science*, *127*,270–276.

Zhao, H. S., Zhang, Y., & Lie, S. T. (2018). Explicit frequency equations of free vibration of a nonlocal Timoshenko beam with surface effects. *Acta Mechanica Sinica*, *34*, 676. https://doi.org/10.1007/s10409-018-0751-6.

Zhen, Y.-X., Wen, S.-L., & Tang, Y. (2019). Free vibration analysis of viscoelastic nanotubes under longitudinal magnetic field based on nonlocal strain gradient Timoshenko beam model. *Physica E: Low-dimensional Systems and Nanostructures*, *105*, 116–124.

Zhu, B., Chen, X., Dong, Y., & Li, Y. (2019). Stability analysis of cantilever carbon nanotubes subjected to partially distributed tangential force and viscoelastic foundation. *Applied Mathematical Modelling*, *73*, 190–209.